Cerebral Cortex July 2014;24:1867–1878
doi:10.1093/cercor/bht037
Advance Access publication February 25, 2013

Illusory and Veridical Mapping of Tactile Objects in the Primary Somatosensory and Posterior Parietal Cortex

Ilaria Bufalari[1,2], Francesco Di Russo[3,4] and Salvatore Maria Aglioti[1,2]

[1]Dipartimento di Psicologia, Università degli Studi di Roma "La Sapienza", I-00185 Rome, Italy, [2]Laboratorio di Neuroscienze Sociali, [3]Centro Ricerche Neuropsicologia, IRCCS Fondazione Santa Lucia, I-00179 Rome, Italy and [4]Dipartimento di Scienze Motorie, Umane e della Salute, Università degli Studi di Roma "Foro Italico", I-00135 Rome, Italy

Address correspondence to Ilaria Bufalari, Dipartimento di Psicologia, Università degli Studi di Roma "La Sapienza", Via dei Marsi 78, I-00185 Rome, Italy. Email: ilaria.bufalari@uniroma1.it.

While several behavioral and neuroscience studies have explored visual, auditory, and cross-modal illusions, information about the phenomenology and neural correlates of somatosensory illusions is meager. By combining psychophysics and somatosensory evoked potentials, we explored in healthy humans the neural correlates of 2 compelling tactuo-proprioceptive illusions, namely Aristotle (1 object touching the contact area between 2 crossed fingers is perceived as 2 lateral objects) and Reverse illusions (2 lateral objects are perceived as 1 between crossed-fingers object). These illusions likely occur because of the tactuo-proprioceptive conflict induced by fingers being crossed in a non-natural posture. We found that different regions in the somatosensory stream exhibit different proneness to the illusions. Early electroencephalographic somatosensory activity (at 20 ms) originating in the primary somatosensory cortex (S1) reflects the phenomenal rather than the physical properties of the stimuli. Notably, later activity (around 200 ms) originating in the posterior parietal cortex is higher when subjects resist the illusions. Thus, while S1 activity is related to illusory perception, PPC acts as a conflict resolver that recodes tactile events from somatotopic to spatiotopic frames of reference and ultimately enables veridical perception.

Keywords: Aristotle illusion, posterior parietal cortex, primary somatosensory cortex, somatosensory evoked potentials, spatial remapping of touch

Introduction

Our history as perceptual agents shapes the way we process information coming from both the internal and external worlds. Experience, thus, plays a fundamental role in building perceptual rules. As a result, physical events that violate normal expectations are typically misperceived. Perceptual illusions arise when a given stimulus, usually delivered under a given condition, induces a different conscious experience when the conditions are changed (Hayward 2008). Thus, illusions hint at the prominence of experience over sensation in adult life. Most of the studies exploring these phenomena focus on the visual modality. Recently, the phenomenology and the neural correlates of visual and cross-modal illusions have been investigated by combining behavioral studies with neuroimaging and neurophysiological studies (Macknik and Haglund 1999; Withney et al. 2003; Ehrsson et al. 2004).

Compelling illusions also occur in the tactile domain (Hayward 2008; Dieguez et al. 2009). One of the most striking somatosensory illusions was first described by Aristotle in his Metaphysica IV, 6 and De Somniis 2 (Aristotle 1924). This illusion, eponymously associated with the great Greek philosopher, requires a person to cross 2 adjacent fingers, one over the other (e.g. the middle over the index finger) and then touch a small object (e.g. one's own nose) using the medial part of the crossed fingertips. In this position, people frequently experience the sensation of touching 2 objects instead of 1 (e.g. the feeling of having 2 noses). Moreover, it has been proven that if 2 different objects are presented to each of the 2 crossed fingertips, then their relative location will be incorrectly perceived (Benedetti 1985). Importantly, accurately perceiving the location of objects that touch the skin requires information about the size and shape of objects and the configuration and posture of the body. Thus, touch and proprioception are inherently linked to the body, and they have to be re-referenced to it. The illusion of double sensation (or "tactile diplopia") and mislocalization may be a consequence of the brain failing to dynamically integrate information regarding the incoming tactile inputs with proprioceptive information about the unusual position of the stimulated body part (Benedetti 1985, 1986a, 1986b). Thus, the brain needs a model of the perceiving body in order to form veridical tactile representations of the outside world. Despite the relevance of tactile diplopia for understanding how the brain remaps touch according to the body's position in space (from somatotopic to external frames of reference; Longo et al. 2010), no studies exploring the neural correlates of the Aristotle illusion have been performed so far. Even more strikingly, only 3 neuroimaging studies have explored 2 purely tactile illusory conditions, namely, the rabbit illusion, using functional magnetic resonance imaging (fMRI) in humans (Blankenburg et al. 2006), and the funneling illusion, using optical imaging (Chen et al. 2003) and high-field fMRI (Chen et al. 2007) in monkeys. Notably, the above studies demonstrate that neural activity in the primary somatosensory cortices (S1s) reflects the perceptual rather than the physical properties of the stimuli.

While a few previous studies suggest that the S1 is activated during purely tactile illusions, 2 fundamental questions remain largely unaddressed. The first concerns the brain regions that are prone to somatosensory illusions and those that can distinguish physical stimulation from phenomenal perception. The second concerns the temporal processing within the neural circuit that is called into play during veridical and illusory processing of somatosensory information. To this aim, we recorded somatosensory evoked potentials (SEPs) from the stimulation of the right median nerve to get a time-locked measure of somatosensory processing during the continuous tactile stimulations of crossed fingers that gave rise to: (1) The Aristotle illusion (illusory doubling of a single stimulus moving along the contact area of the index and middle fingers); (2) the Reverse illusion (illusory merging of 2

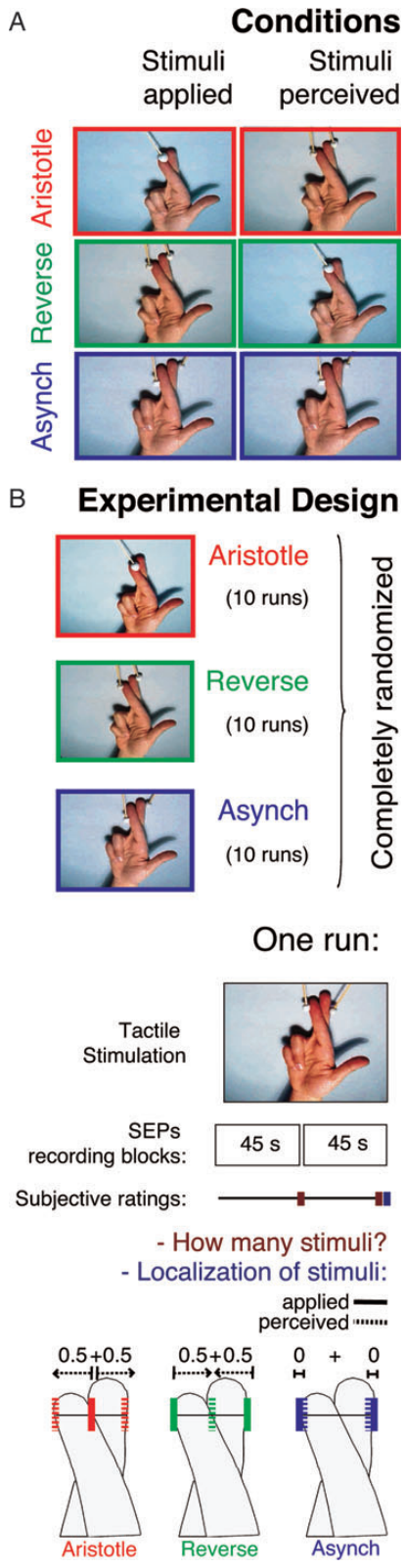

Figure 1. Experimental design. Three tactile stimulation conditions were delivered by moving 1/2 wooden balls along the first phalanx of subjects' right and middle fingers: (*A*) "Applied" and "perceived" indicate the physical stimuli and the phenomenal experience corresponding to them in most of the blocks; (*B*) each of the 3 tactile stimulation conditions consisted of 10 runs. The order of the 30 runs was completely randomized. Each run consisted of two 45-s SEPs recording blocks, separated by a brief pause in which subjects: (1) verbally reported the number of stimuli they felt throughout the block; (2) pencil-marked the perceived position of the stimulus/stimuli on crossed-finger schematic drawings (on a 1-cm horizontal line across the first phalanx of the crossed fingers). This allowed us to measure the distance between the actual (straight lines) and perceived (dashed lines) location of stimuli [scores of 0 were assigned if there was no difference between the actual and perceived location of stimuli (no illusion), while scores of 1 meant this distance was maximal (illusion)].

stimuli moving along the external area of the crossed fingers), which was anecdotally reported by Rivers (1894); and (3) the Asynchronous control nonillusory condition (2 asynchronous tactile stimuli moving along the external area of the crossed fingers are correctly perceived as 2).

Using the median nerve, SEPs technique allowed us to explore the functionality of the somatosensory pathway with high temporal resolution. Indeed, early (at 20–70 ms) and middle/late (70–300 ms) somatosensory components reflect the activity of primary and higher-order somatosensory cortices (Allison et al. 1989; Valeriani et al. 2001). Moreover, the combination of information about the latency, amplitude, and source localization of SEPs provides a unique description of the spatio-temporal dynamics of somatosensory processing and the differential involvement of primary and higher-order somatosensory areas in the occurrence of illusory or veridical percepts. In fact, we recorded the occurrence and amount of mislocalization for each condition on a block-by-block basis (see Materials and Methods and Fig. 1*B*). First, we compared the SEPs in the 3 tactile stimulation conditions, independent of the perceptual outcome. Then, we ran a second step of analyses that allowed us to compare SEPs in the stimulation blocks in which subjects were prone (Aristotle and Reverse illusions) or resisted (Aristotle and Reverse no illusions) the illusions, i.e., when subjects veridically localized the stimuli despite illusory stimulation. The basic logic of this approach was that if a neural process reflects perceived rather than actual stimulation, then the Reverse condition (in which 1 object is perceived) should differ from both the Aristotle and Asynchronous conditions (in which 2 objects are perceived). In contrast, if a neural process reflects the integration of tactile and proprioceptive inputs to come up with veridical percepts, then conditions where this integration is successful (eliciting correct localization, as in Aristotle and Reverse no Illusions) should differ from conditions where this integration is not successful (eliciting incorrect localization, as in Reverse and Aristotle illusions) and from conditions where this integration is not required to reach correct localization (Asynchronous control condition). In this way, we were able to provide new insights about the neural signatures of failure or success in the integration of misaligned proprioceptive and tactile inputs due to a non-natural, finger-crossed posture.

Materials and Methods

Participants

Twenty-two right-handed (Oldfield 1971) healthy volunteers [11 males; 22.9 years old ± 2.9 (mean ± standard deviation)] participated in the study. Participants were naïve as to the purposes of the experiment, and they had never previously experienced the Aristotle and Reverse illusions. Participants gave their written informed consent and were paid €10 per hour for their participation. The procedures were approved by the local ethics committee and were in accordance with the ethical standards of the 1964 Declaration of Helsinki.

Stimuli

Subjects sat in an armchair in a warm room with their right forearm lying supine on a table. A removable strip of tape kept the subjects' fingers crossed. This was placed to avoid any discomfort and/or muscle contraction caused by active maintenance of the non-natural crossed-finger posture. The strip could be removed on request during the intervals between SEPs recording runs, which allowed participants to move their fingers and to avoid cramping sensations. Prior to the experiment, participants were visually presented with 2 wooden balls (6-mm diameter each) connected to a stick and were informed they could be touched by 1 or 2 balls either at the external or the central part of the right middle and index fingers, which were kept in the crossed position (Fig. 1*A*).

An experimenter delivered the tactile stimulation by moving the wooden balls continuously back and forth along the distal phalanx of the crossed fingers and was trained to use the same frequency (about 1.5 cycle/second) and to force across the 3 different types of tactile stimulations. Three stimulation conditions were used: (1) 1 central ball, which was typically perceived as 2 external balls (Aristotle); (2) 2 external synchronous balls, which were typically perceived as 1 ball located at a point between the crossed fingertips (Reverse); (3) 2 external asynchronous balls, which were veridically perceived as 2 external balls (Asynchronous control condition). In the synchronous condition, corresponding fingers' portions were simultaneously touched. In the Asynchronous stimulation, instead, corresponding fingers' portions were touched at different time points (as shown in Fig. 1*A*).

Concomitantly with the tactile stimulations on the crossed fingertips, the SEPs were obtained by nonpainful electrical stimulation of the right median nerve (which innervates the index and middle fingers) at the wrist (constant current square-wave pulses; stimulus intensity was set individually just above the thumb's motor threshold, mean frequency = 1.2 Hz, duration = 0.5 ms, mean intensity = 16.8 mA). To avoid habituation, the interstimulus interval was set randomly between 700 and 900 ms (in steps of 100 ms). An occluding panel was positioned so that the subjects could not see the electrical and the tactile stimulations delivered to their right hand.

Procedure

The experiment lasted approximately 3 h. Participants were instructed not to blink or move the eyes during the SEPs recording session, to continuously pay attention to the location and number of stimuli touching their fingers, and to disregard the electric stimulation applied to their median nerve. Each of the 3 tactile stimulation conditions described above (Aristotle, Reverse, and Asynchronous) was presented in 10 runs (Fig. 1*B*). The order of the 30 runs was completely randomized within each subject. Each run lasted approximately 90 s and included two 45-s blocks of tactile stimulation in a given condition belonging to the same category of stimulation. During each 45-s block of tactile stimulation, the electroencephalogram (EEG) was continuously recorded and the SEPs were evoked by the electrical stimulation of the right median nerve. At the end of the first block, the SEPs recording and the tactile stimulation were stopped to allow the subject to verbally report how many stimuli he/she felt. Participants were asked to answer "1"/"2" if they clearly perceived 1 or 2 stimuli, respectively, and "three" if they were uncertain about the number and/or location of stimuli. At the end of each run, subjects had again to verbally report how many stimuli they felt and to draw their corresponding location on crossed-finger schematic drawings (Fig. 1*B*). If the perceived stimuli location changed from the first to the second block, subjects were asked to report the number and position of the stimuli for each block. Pauses between blocks and runs were introduced to reduce the subjects' fatigue.

SEP Recording

EEG recordings were obtained from 64 tin electrodes, following the 10-10 international system by a BrainVision system. The horizontal and vertical electro-oculograms were recorded by electrodes at right external canthi and below the left eye. As recommended in SEPs recordings, all scalp electrodes were referenced to the right mastoid ipsilateral to the stimulation side to avoid that early SEPs (that typically peak contralateral to the stimulation side) were reduced by the subtraction between active electrodes and the reference. The ground electrode was placed on the forearm ipsilateral to the stimulation side to reduce the artifact due to the electrical stimulation of the wrist (ACNS 2006; Cruccu et al. 2008). Electrode impedances were kept <5 kΩ, and all signals were digitized (rate of 5000 Hz), filtered (1–2000 Hz), and stored on a disk for off-line averaging. Semiautomatic artifact rejection was performed by an experimenter blind to the conditions, prior to signal averaging in order to discard epochs containing transients exceeding 90 μV at any recording channel. On average, about 18% of the trials were rejected in each condition. The EEG was segmented for each electrical stimulus giving epochs of 600 ms (−100 to 500 ms). The baseline was calculated from 100 to 0 ms before the electrical stimulus. The averages were digitally band-pass filtered between 1–100 (to analyze early SEPs) and 1–40 Hz (to analyze middle/long-latency SEPs).

Data Analysis

Subjective Reports

Subjective measures concerning the perceived number and localization of the stimulus/stimuli were analyzed separately. Blocks in which subjects reported "2" after Aristotle stimulation or "1" after Reverse and Asynchronous stimulations were indexed as illusory perception. The rare blocks where subjects reported "3"—that is, uncertainty about the number/localization of stimuli—were not included in the statistical analyses (a total of 8 blocks after Aristotle, 4 after Asynchronous, and 2 after Reverse stimulation).

The frequency of illusory percepts was analyzed by means of repeated-measures analysis of variance (ANOVA) with the type of stimulation as a within-subject factor (3 levels: Aristotle, Reverse, and Asynchronous).

As a measure of illusory localization, the distance between actual and subjectively perceived location of stimuli (pencil-marked on a 1-cm horizontal line over the first phalanxes of crossed fingers in the schematic hand drawings) was computed. Scores could vary between 0 and 1. A score of "0" was assigned if there was no difference between the actual and the perceived location of stimuli (no illusion), while a score of 1 indicates the maximal possible mislocation (illusion). More specifically, for the Aristotle stimulation condition, a mark at the contact point of the crossed fingers was scored as 0 (=no illusion). Marks at the noncontact points were scored between 0 and 0.5. Thus, the maximal possible score was 1 (0.5 cm at right plus 0.5 cm at the left with respect to the centre of the line). In the case of Reverse and Asynchronous stimulations, 2 marks at the outer external side of crossed fingers were calculated as 0 (=no illusion), while 1 mark in the exact centre of the fingers was calculated as 1 (illusion; Fig. 1*B*).

Localization scores were entered in 1-way repeated-measures ANOVA, with condition as the main effect (with 5 levels: Aristotle illusion, Reverse illusion, Aristotle no illusion, Reverse no illusion, and Asynchronous).

Electrophysiological and Source Analyses

Grand averages of SEPs recorded in the different stimulation conditions were obtained. Typical early, middle, and long-latency SEP components were identified on the basis of their topographical distribution, by means of scalp voltage maps, and labeled on the basis of latency and polarity (Allison et al. 1989; Valeriani et al. 2001). As is common in SEPs recordings, for early latency SEP components (N20, N30, P45, and N60), peak amplitudes were measured from prestimulus baseline. For middle/long-latency components, mean amplitude of the area beneath the curve was computed within specific time windows centered around the peak of each component, with respect to the mean voltage of a 100-ms prestimulus baseline (P100: 90–110 ms; N120: 114–134 ms; P200: 180–240 ms; and P300: 240–320 ms). Three-dimensional (3D) topographical spline interpolation maps of scalp voltage distribution were obtained using the Brain Electrical Source Analysis (BESA 2000, system version 5.18).

Statistical analyses on the SEP components were run first by taking into account the different tactile stimulation conditions (Aristotle, Reverse, and Asynchronous) and then by comparing the blocks

where subjects were prone or resisted the illusions (Aristotle illusion, Aristotle no illusion, Reverse illusion, Reverse no illusion, and Asynchronous). This second procedure allowed us to uncover SEP modulations related to veridical versus illusory perception.

Analyses Based on the Tactile Stimulation Condition

For each early component, a repeated-measures 1-way ANOVA with the stimulation condition as a factor ("Aristotle", "Reverse", and "Asynchronous") was conducted on individual peak amplitude and latency values. For each component, the mean of the 2 adjacent electrodes with greater amplitude was used.

For each middle and long-latency component, repeated-measures 2-way ANOVAs with the stimulation condition (Aristotle, Reverse, and Asynchronous) and electrode (3 levels) as main factors were conducted on individual area amplitude and peak latency values. Three groups of electrodes with greater amplitude were selected. The mean amplitude of the 3 electrodes was used for each group.

The selection of peak electrodes was guided by the evaluation of scalp topographies in group-averaged data. All post hoc analyses were carried out by means of the Newman–Keuls test. One subject who did not show a clearly recognizable waveform and topography on the N20 SEP component was excluded from the statistical analysis relative to this component.

Analyses Based on Perceptual Judgment

In the N20 and the P200 components where a significant main effect of stimulation condition was initially found, blocks during which subjects felt or resisted the illusions were separately averaged for the 2 illusion conditions.

Importantly, the early N20 is a very small amplitude component. This implies that many hundreds of artifact-free responses have to be averaged to obtain a good signal-to-noise ratio and to extract the N20 component from background noise. Given the high occurrence of illusory percepts (see Results section), the number of artifact-free responses in nonillusory blocks was not enough to obtain a clear N20 component. However, to run statistical analyses based on perceptual judgments also for the N20 component, we compared the illusory percepts in the subsample of subjects who were highly prone to the illusions (occurrence of both illusions in at least 60% of the blocks). This procedure allowed us to have a subsample of subjects ($n = 12$) with a number of artifact-free responses sufficient to have a good signal-to-noise ratio also when separating illusory versus nonillusory blocks. As a consequence of the same above-mentioned reasons, we could not run the analyses on the N20 in the no-illusion conditions (as we did for the P200).

For the P200 component, repeated-measures ANOVAs were conducted on area amplitude values with the factor condition including 5 levels (Aristotle illusion, Reverse illusion, Asynchronous, Aristotle no illusion, and Reverse no illusion). For the Asynchronous condition, the few blocks in which subjects reported the illusion of perceiving the 2 asynchronous stimuli as one (<10% of total blocks) were not included in the statistical analysis. Subjects who always (100% of runs) experienced both the Aristotle ($n = 4$) or Reverse ($n = 3$) illusions could not be included in the comparisons that included the Aristotle no illusion or Reverse no illusion conditions. Similarly, participants who never experienced Aristotle ($n = 1$) or Reverse ($n = 2$) illusions could not be included in the comparisons that included the Aristotle illusion or Reverse illusion conditions.

Since in both the Aristotle and Reverse conditions, nonillusory blocks were less than illusory ones, a signal-to-noise ratio may in principle be lower in the no-illusion conditions and thus result in artificially higher components (Thomas et al. 2004) if peak amplitudes were used. Therefore, we calculated the mean amplitude voltage for each waveform in the time window of interest. This procedure is recommended to eliminate any bias due to differences in the signal-to-noise ratio and is the gold standard for comparing conditions resulting from a different amount of artifact-free responses (Luck 2005).

Source Analysis

For significantly different SEP components, estimation of their intracranial sources was carried out using the BESA 2000. We used the spatiotemporal source analysis of BESA that estimates location, orientation, and time course of multiple equivalent dipolar sources by calculating the scalp distribution obtained for a given model (forward solution). This distribution was then compared with that of the actual SEPs. Interactive changes in source location and orientation lead to the minimization of residual variance between the model and the observed spatiotemporal SEP distribution. The 3D coordinates of each dipole in the BESA model were determined with respect to the Talairach axes (Talairach and Tournoux 1988). In these calculations, BESA assumed a realistic approximation of the head (based on the MRI of 24 subjects). The possibility of interacting dipoles was reduced by selecting solutions with relatively low dipole moments with the aid of an "energy" constraint (weighted 20% in the compound cost function, as opposed to 80% for the residual variance). The optimal set of parameters was found in an iterative manner by searching for a minimum in the compound cost function. Latency ranges for fitting were chosen (N20: 19–20 ms and P200: 185–235 ms) to minimize overlap among successive, topographically distinctive components. To compare source localization across conditions, the model was calculated for each subject. Differences in source localization were also evaluated by means of separated 1-way repeated-measures ANOVAs: (1) On the Euclidean distance between the 3 stimulation conditions (3 levels: Aristotle–Reverse, Aristotle–Asynchronous, and Reverse–Asynchronous conditions); and (2) on the Euclidean distance between illusory and nonillusory trials within each illusory stimulation condition (e.g., Aristotle illusion vs. Aristotle no illusion; Reverse illusion vs. Reverse no illusion). Post hoc comparisons were carried out by means of the Newman–Keuls test.

Correlation Analysis Between Electrophysiological Data and Subjective Reports

To explore whether SEPs modulation contingent upon Aristotle and Reverse conditions was related to the strength of the illusory percept, we carried out correlational analyses between subjective reports and the SEP components in which a specific illusory-related modulation was found.

Results

Subjective Reports

Both Aristotle and Reverse conditions were effective in producing illusorily mislocalized percepts as shown by: (1) The significantly higher number of illusory reports after Aristotle and Reverse stimulations with respect to Asynchronous control [Frequency: $F_{2,42} = 36.46$, $P < 0.00001$; Aristotle (mean ± standard error of the mean, SEM : 73 ± 6%) and Reverse (62 ± 7%) condition versus Asynchronous (10% ± 4), all Ps = 0.0001; Aristotle versus Reverse stimulation, $P = 0.15$; Fig. 2*A*]; (2) significantly higher distances between actual and perceived location of stimuli in illusory versus veridical perception ($F_{4,84} = 55.08$, $P < 0.00001$; Aristotle and Reverse illusion conditions > Aristotle and Reverse no illusion conditions and of control Asynchronous condition; see Fig. 1*B* and Materials and Methods for explanations on how distance was computed). Interestingly, illusory merging of tactile stimuli (Reverse illusion; mean ± SEM: 0.91 ± 0.06) resulted in higher mislocalization than illusory doubling of a single touch (Aristotle illusion; 0.60 ± 0.03) [all comparisons: Ps < 0.0001, except for Asynchronous (0.33 ± 0.03) and Reverse no illusion (0.32 ± 0.05) conditions, in which 2 tactile stimuli were perceived at the same lateral location, $P = 0.81$; Fig. 2*B*].

Electrophysiological and Source Analysis Data

Statistical analyses on the amplitudes/latencies of early and middle/long-latency components showed no significant main or interaction effects for all the examined components

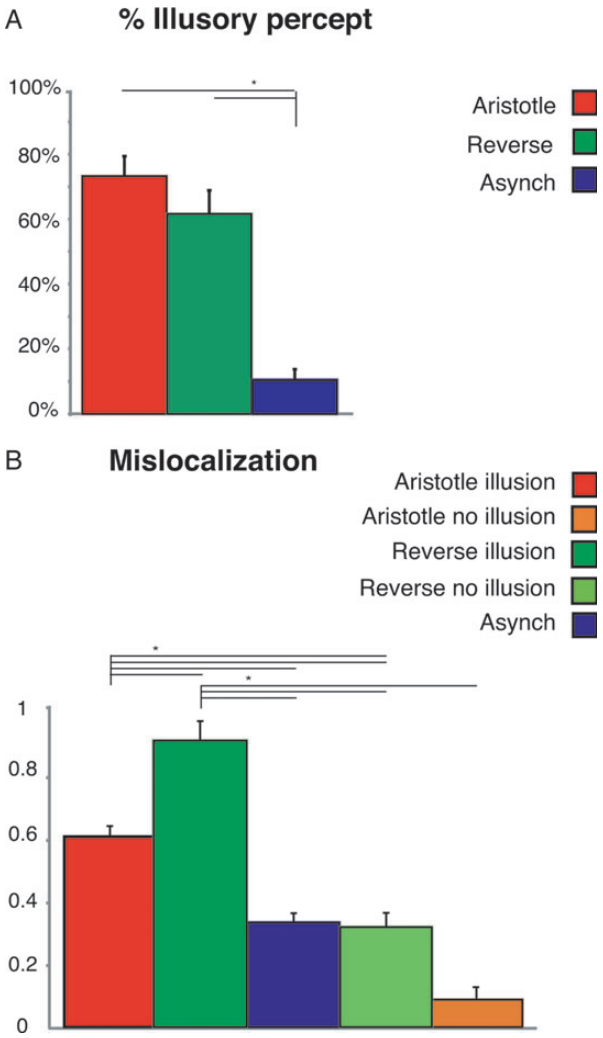

Figure 2. Subjective measures indexing perceptual experience concerning stimulus number and location in the different stimulation conditions. (*A*) Frequency of illusory percepts (expressed as a percentage of total stimulation blocks). (*B*) Distance between the actual and perceived location of stimuli in blocks where subjects were prone (Aristotle and Reverse illusions) or resisted the illusory stimulations (Aristotle and Reverse no illusions) and in the control condition (Asynchronous). Distances could vary between 0 and 1. Scores of 0 were assigned if there was no difference between the actual and perceived location of stimuli (no illusory mislocation). Scores of 1 indicate maximal mislocation distance (and corresponded to 1 cm on the line). Mean and standard errors are reported. Asterisks indicate significant differences across conditions.

(all $Ps > 0.05$), with the exception of N20 and P200 components. Results for these components are reported in the following paragraphs.

Early Activity Originating in the Primary Somatosensory Cortex Reflects Illusory Rather Than Physical Features of the Stimuli

Extensive and detailed somatic representation of fingers in the standard anatomical position takes place in the posterior wall of the postcentral gyrus (corresponding to area 3b of S1) according to homuncular rules (with the thumb located laterally, anteriorly and inferiorly to the little finger; Penfield and Boldrey 1937). The question arises as to whether somatotopic maps in S1 are updated according to the new position of the crossed fingers. Indeed, crossing fingers brings into the proximity portions of the skin that are normally distant in an anatomical position. If updating of somatotopic maps occurs, proximal areas in S1 will respond to stimuli delivered to finger areas that are close to each other in the crossed, but not in the anatomical, finger position. Otherwise, proximal areas in S1 will respond to stimuli delivered to finger areas that are adjacent in the anatomical, but not in the crossed, finger position. In the first case, components indexing S1 neural activity should be similar for the Reverse and Asynchronous conditions where, despite different perceptual reports of 1 central versus 2 lateral stimuli, the physical stimuli are always 2 lateral. In contrast, if the second hypothesis is true, similar S1 neural activity should be found for both the Aristotle and Asynchronous conditions where, despite the different physical stimulation, subjects reported the same perceptual experience of 2 lateral stimuli.

Analyses Based on Tactile Stimulation Conditions

N20 Amplitude Analysis. One-way repeated-measures ANOVA on the amplitude of N20, a component mainly detected at parietal electrodes contralateral to the sensory stimulation (P5-CP5) and thought to be generated in the area 3b of the S1 (area S1) (Allison et al. 1989; Valeriani et al. 2001), showed a significant main effect of the stimulation condition ($F_{2,40} = 6.02$, $P = 0.005$). As shown by the Newman–Keuls post hoc comparisons, N20 amplitude was significantly enhanced in the Reverse stimulation condition, which mostly gave rise to illusory perception of one stimulus, with respect to Asynchronous and Aristotle stimulations, which gave rise to veridical and illusory perception of 2 stimuli [Reverse (mean ± SEM): -1.2 ± 0.11 versus Asynchronous (-0.97 ± 0.1, $P = 0.009$) and Aristotle (-0.98 ± 0.12, $P = 0.007$)], respectively. No N20 amplitude differences between Aristotle and Asynchronous stimulations were found ($P = 0.798$). Peak amplitudes and topographic distribution are shown in Figure 3*A*,*B*.

N20 Source Analysis. N20 sources were localized in the left contralateral S1 in area 3b (Talairach coordinates of the N20 sources are shown in Fig. 3*C*). The residual variance of the source models in the 19- to 20-ms interval was $2.62 \pm 0.43\%$ (mean ± SEM) for Aristotle, $2.85 \pm 0.47\%$ for Reverse, and $3.04 \pm 0.41\%$ for Asynchronous stimulation. It is worth noting that the N20 source in the Reverse stimulation was localized more dorsally than the other 2 conditions ($F_{2,40} = 12.71$, $P = 0.00005$). The Euclidean distance between the Reverse and Aristotle stimulations (mean ± SEM: 10.38 ± 1.28 mm), and the Reverse and Asynchronous stimulations (10.10 ± 1.28 mm), was significantly greater than the distance between the Aristotle and Asynchronous stimulations [(6.86 ± 0.98 mm); both $Ps = 0.0003$].

Analysis Based on Perceptual Judgment

N20 Amplitude Analysis. One-way repeated-measures ANOVA (3 levels: Aristotle illusion; Reverse illusion; and Asynchronous) on the subset of subjects particularly prone to the illusions confirmed the pattern of results obtained on the entire sample, even when the contribution of nonillusory trials was removed. The significant main effect of the condition ($F_{2,22} = 4.64$, $P = 0.02$) was due to enhanced N20 amplitudes for Reverse illusion [mean ± SEM: -1.11 ± 0.12

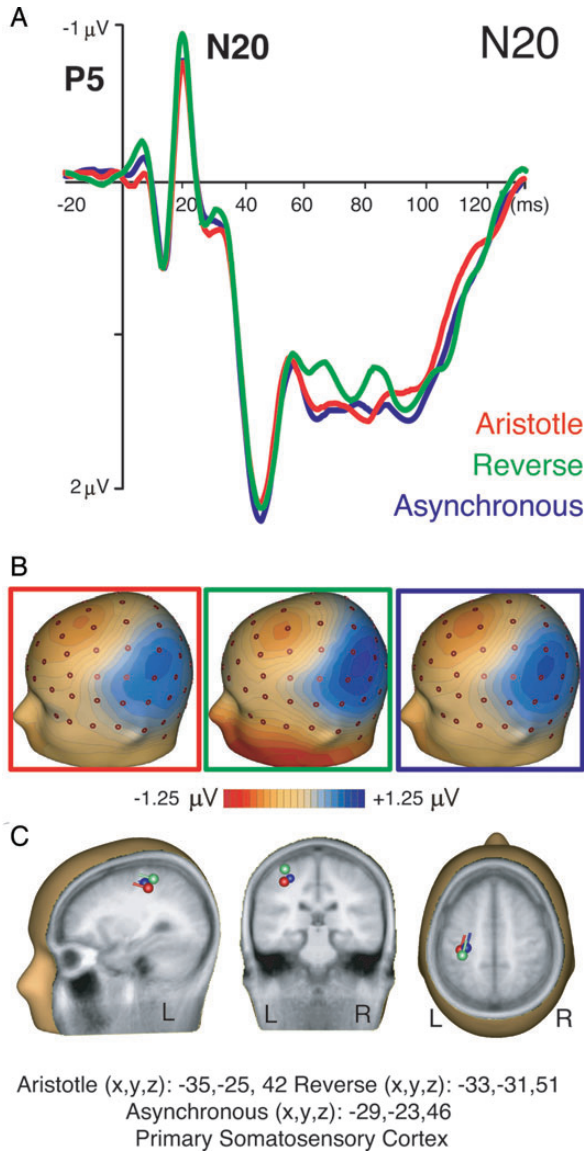

Figure 3. Modulations of N20 reflect phenomenal experience. (*A*) Waveforms, (*B*) scalp distribution, and (*C*) source location (with Talairach coordinates values for *x*-, *y*-, and *z*-axes) of the N20 component in the 3 tactile stimulation conditions are reported. One stimulus perception following Reverse tactile stimulation resulted in significant higher amplitudes and more dorsal source locations in the left S1, with respect to 2 stimuli perception resulting from Aristotle and Asynchronous stimulations.

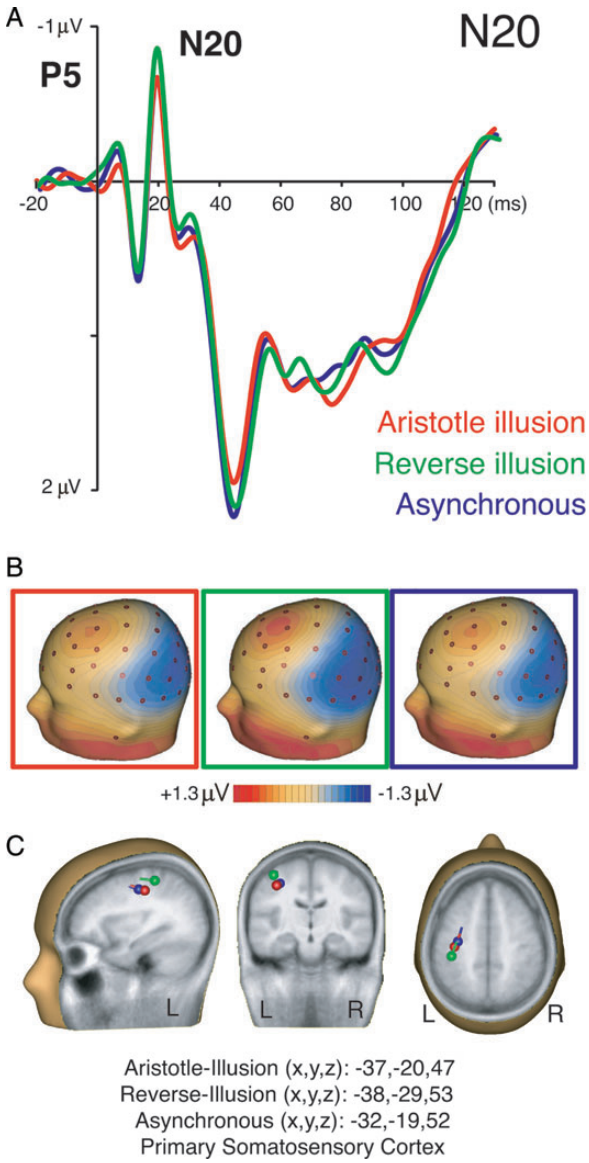

Figure 4. Modulations of N20 reflect phenomenal experience even when the contribution of nonillusory trials is removed. (*A*) Waveforms, (*B*) scalp distribution, and (*C*) source locations (Talairach coordinates values for *x*-, *y*-, and *z*-axes) of the N20 component are reported in the subset of subjects particularly prone to the illusions ($n = 12$). Amplitudes and source locations within the left S1 were significantly different in the Reverse than in Aristotle illusion and Asynchronous control conditions.

with respect to both Aristotle illusion (-0.83 ± 0.14, $P = 0.021$) and Asynchronous control condition (-0.86 ± 0.15, $P = 0.035$; see Fig. 4*A*,*B*)].

N20 Source Analysis. Results confirmed that N20 sources were localized in the left contralateral S1 in area 3b (Talairach coordinates of the N20 sources are shown in Fig. 4*C*). The residual variance of the source models in the 19- to 20-ms interval was $3.51 \pm 0.51\%$ (mean ± SEM) for Aristotle illusion, $3.34 \pm 0.56\%$ for Reverse illusion, and $3.58 \pm 0.59\%$ for Asynchronous conditions.

Even when the contribution of nonillusory trials was removed, N20 source in the Reverse illusion was localized more dorsally than in the other 2 conditions ($F_{2,22} = 6.57$, $P = 0.006$). The Euclidean distance between the Reverse illusion and Aristotle illusion (mean ± SEM: 11.5 ± 1.99 mm), and Reverse illusion and Asynchronous condition (11.75 ± 1.88 mm), was significantly greater than the distance between the Aristotle illusion and Asynchronous condition (6.92 ± 1.32 mm; $P = 0.006$ and 0.011).

Late Activity Originating in Higher-Order Somatosensory Cortices Reflects the Somatosensory Integration Processes that Lead to Veridical Versus Illusory Perception

Analyses Based on Tactile Stimulation Conditions

P200 Amplitude analysis. Among the middle/late-latency SEP components, the only significant effects concerned the

P200 component. ANOVA on P200 amplitudes showed significant main effects of condition ($F_{2,42} = 7.74$, $P = 0.001$) and electrode ($F_{2,42} = 5.47$, $P = 0.008$). Importantly, their interaction was significant ($F_{4,84} = 2.48$, $P = 0.049$). Post hoc comparisons showed higher amplitudes in both Aristotle and Reverse than in the Asynchronous stimulation condition at central, frontal, and posterior sites (Aristotle vs. Asynchronous, all $Ps \leq 0.0001$; Reverse vs. Asynchronous, all $Ps \leq 0.0001$; see Fig. 5*A*,*B* and Table 1).

P200 Source Analysis. The P200 component was modeled by a dipole localized in the left contralateral parietal area within the inferior parietal lobule (area 40, Talairach coordinates of the P200 sources are shown in Fig. 5*C*). The residual variance of the source models in the 185- to 235-ms time intervals was 3.74 ± 0.62% (mean ± SEM) for Aristotle, 4.21 ± 0.59% for Reverse, and 4.56 ± 0.54% for Asynchronous control conditions.

The ANOVA on the Euclidean distance between the P200 source localizations showed significant differences among conditions ($F_{2,42} = 17.77$, $P = 0.000003$). Post hoc tests indicated that the source for the Asynchronous stimulation was localized more dorsally than the 2 illusory stimulations. Indeed, the distance between the Reverse and Asynchronous stimulations (mean ± SEM: 12.64 ± 2.09 mm), and between the Aristotle and Asynchronous stimulations (13.86 ± 2.15 mm), were both significantly greater than the distance between the Aristotle and Reverse stimulations (4.45 ± 0.80 mm, both $Ps = 0.0001$).

Analysis Based on Perceptual Judgment

P200 Amplitude Analysis. Importantly, to tell apart possible differences related to illusory versus veridical perceptions, we analyzed separately the blocks in which subjects felt or resisted the illusions (see Materials and Methods). Results confirmed significant higher amplitudes at central sites in both the Aristotle and Reverse illusory conditions with respect to the control Asynchronous condition (significant interaction "Condition × Electrode": $F_{8,88} = 3.26$, $P = 0.002$; Aristotle illusion vs. Asynchronous, $P = 0.038$; Reverse illusion vs. Asynchronous, $P = 0.0007$; Aristotle vs. Reverse illusion, $P > 0.05$; see Table 2). Interestingly, P200 amplitude was higher in nonillusory than in illusory perception blocks (Aristotle no illusion vs. Aristotle illusion at central and posterior sites: all $Ps < 0.0001$; Reverse no illusion vs. Reverse illusion at frontal, central, and posterior sites: all $Ps < 0.0002$). The same effect was found with respect to the control Asynchronous condition (Aristotle and Reverse no illusions vs. Asynchronous at either frontal, central, or posterior sites, all $Ps < 0.002$, Fig. 6*A*,*B*).

P200 amplitude was different even when the number of perceived stimuli was identical, thus regardless the amount of tactile stimuli. Indeed, this component was higher in the Aristotle no illusion than in Reverse illusion condition even though 1 stimulus was perceived in both conditions (at both central and posterior sites, all $Ps < 0.002$). By the same token, P200 amplitude was higher in Reverse no illusion than in Aristotle illusion (at all sites, all $Ps < 0.0001$; Table 2) even though 2 stimuli were perceived in both conditions. These results suggest that P200 is related to the somatosensory integration processes that lead to illusion-prone or veridical responses in conflicting situations rather than to illusory perception per se. Also, it is worth noting that P200 amplitude was higher in the Reverse no illusion with respect to the Aristotle no illusion blocks (all $Ps \leq 0.05$, at frontal and central electrodes).

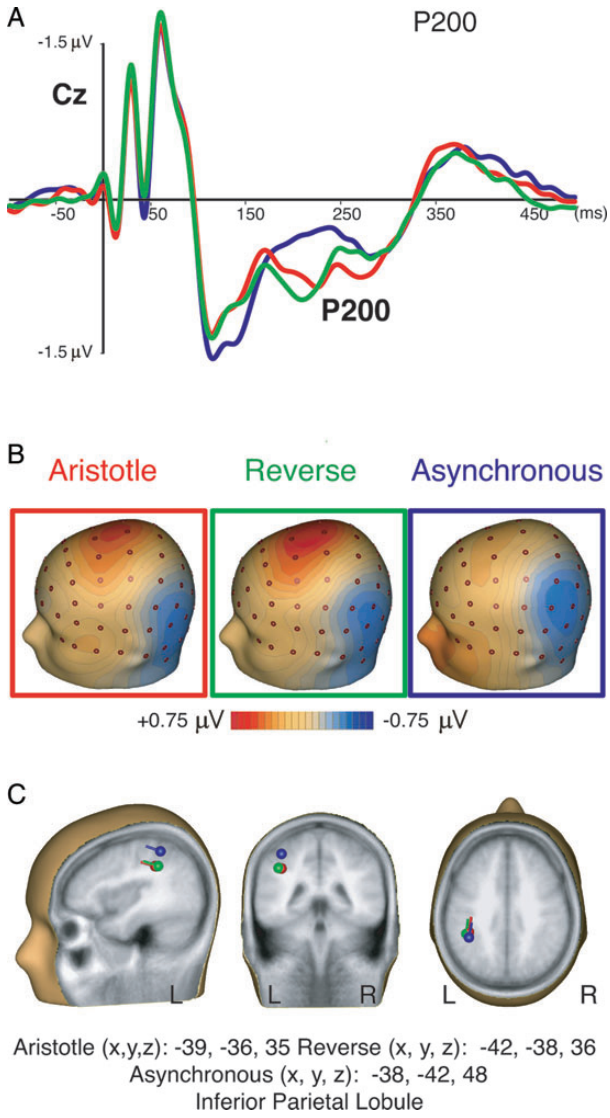

Figure 5. Modulations of P200 as a function of Aristotle and Reverse illusory stimulation conditions. (*A*) Waveforms, (*B*) scalp distribution, and (*C*) source locations (with Talairach coordinates values for *x*-, *y*-, and *z*-axes) of P200 component are reported. Amplitude and source locations within the inferior parietal cortex were significantly different in the Aristotle and Reverse with respect to the Asynchronous stimulation condition.

Table 1
P200 amplitudes in the 3 tactile stimulation conditions

P200	Aristotle	Reverse	Asynchronous
FC1–FCz–FC2			
Mean	0.65	0.69	0.41
SEM	0.14	0.16	0.13
C1–Cz–C2			
Mean	0.66	0.67	0.32
SEM	0.18	0.19	0.16
CP1–CPz–CP2			
Mean	0.41	0.37	0.09
SEM	0.19	0.19	0.18

Note: Mean area amplitudes (±SEM) and peak electrodes for P200 in Aristotle, Reverse, and Asynchronous stimulation conditions.

P200 Source Analysis. Modeling the cortical sources of the P200 confirmed that it originates in the inferior parietal lobule (area 40, Talairach coordinates are shown in Fig. 6*C*).

Table 2
P200 amplitudes as a function of veridical and illusory perception

P200	Aristotle Illusion	Aristotle No Illusion	Reverse Illusion	Reverse No Illusion	Asynchronous No Illusion
FC1–FCz–FC2					
Mean	0.59	0.72	0.64	0.93	0.52
SEM	0.20	0.19	0.22	0.31	0.19
C1–Cz–C2					
Mean	0.66	0.96	0.70	1.06	0.53
SEM	0.24	0.24	0.31	0.31	0.25
CP1–CPz–CP2					
Mean	0.50	0.85	0.50	0.84	0.42
SEM	0.25	0.25	0.31	0.27	0.26

Note: Mean area amplitudes (±SEM) and peak electrodes for P200 separated for veridical and illusory perception in the different stimulation conditions: Aristotle illusion, Aristotle no illusion, Reverse illusion, Reverse no illusion, and Asynchronous no illusion. It is worth noting that amplitudes in the nonillusory blocks are significantly larger than in the illusory ones.

The residual variance of the source models in the 185- to 235-ms interval was 4.13 ± 0.85% (mean ± SEM) for Aristotle illusion, 4.67 ± 0.91% for Aristotle no illusion, 4.5 ± 0.95% for Reverse illusion, and 4.12 ± 0.68% for Reverse no illusion conditions. Importantly, there was a significant shift in the dipole location as a result of veridical versus illusory perception. For the Aristotle illusion condition, the P200 was localized more lateral, anterior, and ventral than the P200 in the Aristotle no illusion condition [$F_{1,15} = 31.00$, $P = 0.00005$; Euclidean distance: 11.38 ± 2.04 mm (mean ± SEM)]. For the Reverse illusion condition, the P200 was localized more medial, anterior, and dorsal than in the P200 Reverse no illusion condition ($F_{1,16} = 33.64$, $P = 0.00003$; Euclidean distance: 11.94 ± 2.06 mm).

Correlation Analysis Between Electrophysiological Data and Subjective Reports

N20 Correlation Analyses. No significant correlation was found between the amplitude of this early SEP component and the subjective measures on the strength of the illusion.

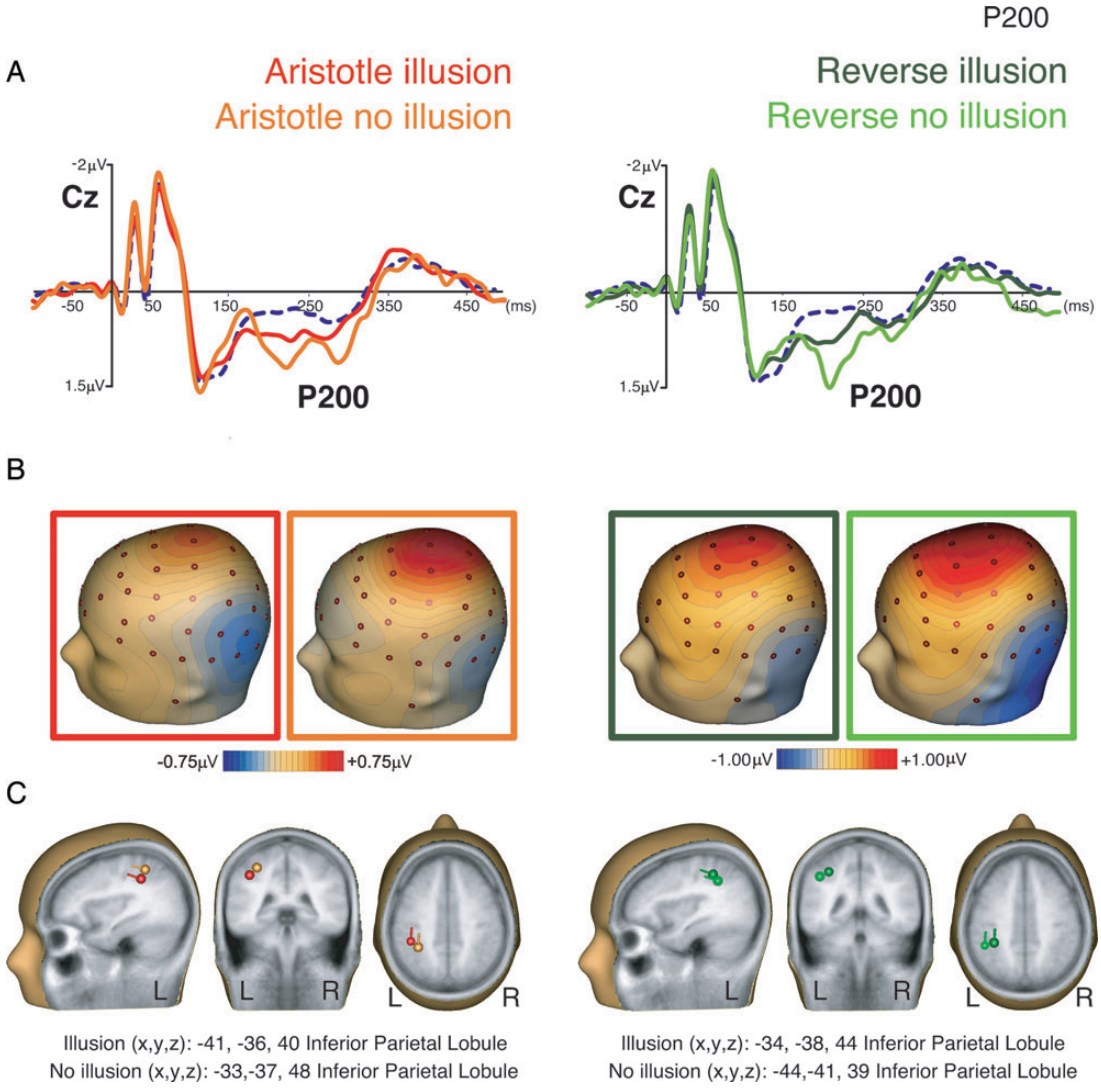

Figure 6. Modulations of P200 reflect veridical and illusory perception in the different stimulation conditions. (*A*) Waveforms, (*B*) scalp distribution, and (*C*) source location of P200 component (with Talairach coordinates values for *x*-, *y*-, and *z*-axes) are represented as function of veridical or illusory subjective reports in the Aristotle (left panel) and Reverse (right panel) stimulation conditions. As a reference, the waveforms relative to the Asynchronous control condition are represented as dashed blue lines.

P200 Correlation Analyses. Separate standard correlations between P200 amplitude and subjective reports about the perceptual experience in the different conditions allowed us to explore the link between neurophysiological and behavioral markers of illusory perceptions. Tellingly, the higher the frequency and the mislocalization of illusory percepts, the smaller the P200 amplitude when subjects were illusorily stimulated [Aristotle stimulation: Frequency: $r = -0.40$, $P = 0.06$; mislocalization: $r = -0.51$, $P = 0.015$, Reverse stimulation: Frequency: $r = -0.47$, $P = 0.028$; mislocalization: $r = -0.44$, $P = 0.04$], and effectively experienced the illusions (R and P values are reported in Fig. 7; all Ps < 0.03, with the exception of correlation between Aristotle illusion and frequency of illusory percepts, $P = 0.06$).

No significant correlations were found between P200 amplitudes in both Aristotle and Reverse no illusion conditions and any of the subjective measures.

Discussion

Here, we explored the Aristotle and the Reverse somatosensory illusions and highlighted, for the first time ever, their neural signatures. While the Aristotle illusion has been investigated at the phenomenal level in previous studies (Benedetti 1985, 1986a, 1986b) only one ancient, anecdotal instance of the Reverse illusion has been reported (Rivers 1894). In the Aristotle illusion, under finger-crossed posture, a single object touches parts of the fingers that in the standard anatomical position can only be touched simultaneously if 2 objects are used. Perceptual learning that occurs, over years of experience, in the anatomical finger positioning creates an alignment between tactile and proprioceptive information. The temporary crossing of the fingers induces a mismatch between these 2 types of information, which is likely the basis of the Aristotle's illusion.

As a matter of fact, changing the typical pattern of finger–object interaction by keeping the finger crossed for up to 6 months may eliminate the illusory doubling of a single stimulus delivered to crossed fingertips (Benedetti 1991). This interpretation of the Aristotle illusion brought us to explore whether synchronous stimulation delivered to external portions of crossed fingers (that in the anatomical position are next to each other) produced the illusory feeling of a unique central stimulus. As demonstrated in our results, we were able to produce this complementary Reverse illusion.

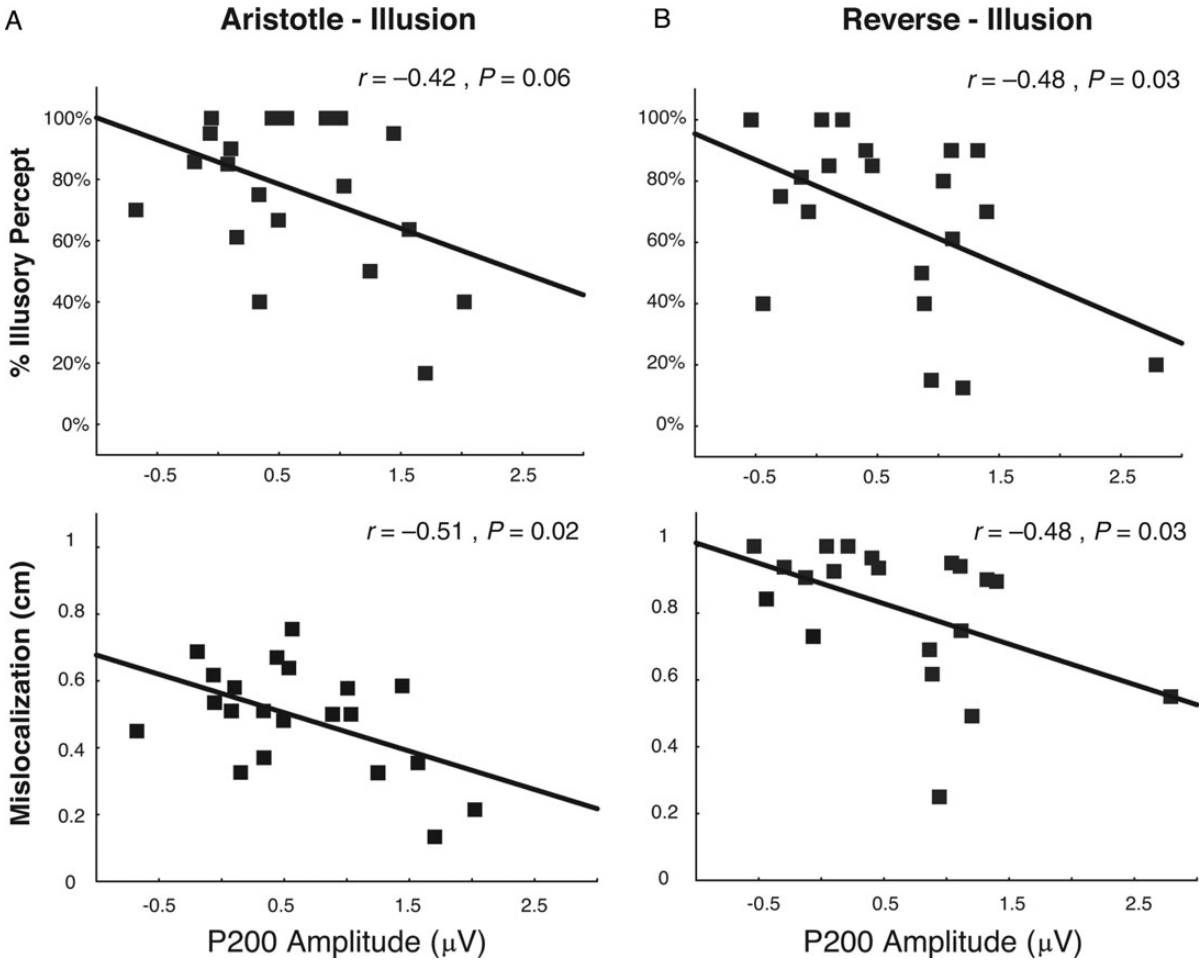

Figure 7. P200 amplitudes vary as a function of the subjective strength of the illusions. Scatterplots show inverse relation between illusion strength (as inferred by the frequency of illusory percepts and distance between the actual and perceived location of the stimuli) and P200 amplitudes in (*A*) Aristotle and (*B*) Reverse illusory blocks. *R*-values and associated *P*-values are reported at the upper right corner of each graph. Importantly, resisting the illusion resulted in significant larger amplitude of P200, suggesting that neural activity in the inferior parietal lobule plays a crucial role in resolving the conflict between tactile and proprioceptive inputs and thus leads to veridical perception.

Recording SEPs evoked by median nerve stimulation—instead of by the continuous tactile stimulation of the fingers—provides the advantage of having clearly synchronized responses, precisely time-locked to the electrical stimulus (Cruccu et al. 2008). Thanks to this procedure, we have been able to obtain baseline measures of early and late somatosensory processing and to test the influence of illusory versus nonillusory tactile stimulation of the fingers on the modulation of amplitude, latency, and dipole locations of early and late SEP components.

Thus, and perhaps more importantly, neurophysiological data allowed us to explore the differential involvement of the S1 and of a multisensory parietal region when conscious somatic perception is driven by physical or phenomenal qualities of the sensory stimuli.

Phenomenal Mapping of Touch in the Primary Somatosensory Cortex

One important result of this study is that early activity in S1 seems to be modulated by the phenomenal instead of the physical features of stimuli. Indeed, N20 amplitude and its dipole location were significantly different in the Reverse (2 lateral stimuli evoking the illusory perception of 1 central stimulus) than in the Aristotle (1 central stimulus perceived illusorily as 2 lateral stimuli) and the Asynchronous (2 lateral stimuli perceived and localized correctly) stimulation conditions. It is worth noting that enhanced N20 amplitude reflects increased excitation in area 3b of S1 (Valeriani et al. 2001). Moreover, N20 amplitude is higher when subjects report the evoking stimuli as mostly intense (Hashimoto et al. 1988). Although delivered manually, the intensity of the physical stimulation was comparable at least in the Reverse and Asynchronous condition. Thus, the observed pattern of N20 amplitude and the resulting dipole localization is likely due to illusory perception rather than a difference in low-level properties of the tactile stimulation in the different conditions. Similar to the funneling illusion, the illusory merging of 2 separate stimuli into a single one results in increased intensity of the perceived stimulus (Gardner and Spencer 1972; see also Supplementary Materials). This is in keeping with optical imaging studies in monkeys that showed simultaneous tactile stimulation of 2 adjacent digits produced a single focus of cortical activation in area 3b, located between the 2 activation foci that are found when the same digits are stimulated separately (Chen et al. 2003). The area of funneled activity was smaller relative to single digit activations, suggesting that increased sensation intensity is encoded by a sharpened focus of cortical activation (Chen et al. 2003; Simons et al. 2007). Indeed, as previously suggested, intensity may occur as a result of strengthening the central stimulation site and masking the peripheral sites (Gardner and Spencer 1972; Gardner and Costanzo 1980). Thus, it is plausible that Reverse stimulation gave rise to a more intense percept (see also Supplementary Materials), which brought about increased N20 amplitude, and a single focus of activation in S1. In contrast, Asynchronous and Aristotle conditions might have induced less intense percepts and 2 discrete foci of neural activity. Congruently, psychophysical observations showed that when 2 stimuli are spaced sufficiently apart, they are perceived as 2 separate stimuli, each weaker in intensity than a single funneled stimulus (von Bekesy 1967; Gardner and Spencer 1972). In sum, congruent with the only 3 studies on the neural correlates of purely tactile illusions performed thus far (Chen et al. 2003, 2007; Blankenburg et al. 2006), our data indicate that topographic activity in S1 reflects phenomenal more than physical features of sensory stimuli, suggesting that this structure is not involved in the process of gaining veridical perceptions connected to touch remapping.

A Tactile-Proprioceptive Conflict Resolver in the Posterior Parietal Cortex

In a number of daily life circumstances, like haptic exploration and goal directed actions in the proximal space, tactile stimuli, which are initially coded according to somatotopic reference frames, have to be localized in external space. This translation from somatotopic into spatiotopic coordinate systems implies that mere tactile information has to be integrated with proprioceptive information about the posture of the stimulated body part. A transcranial magnetic stimulation study on the ability to compare the position in space of facial touches with respect to touches on an arm held in different spatial positions (and thus requiring the use of an external reference frame) indicates that the posterior parietal cortex (PPC) plays an important role in the process of remapping touch in spatiotopic coordinates (Azañón et al. 2010). Moreover, behavioral studies show that, immediately after stimulation, touch is remapped into external space on the basis of a stored representation of the canonical posture, and that the actual position of the body is only subsequently integrated [as in temporal order judgments for tactile stimuli applied to crossed or uncrossed hands and fingers (Yamamoto and Kitazawa 2001; Craig and Busey 2003; Azañón and Soto-Faraco 2008; but see also Shore et al. 2002).

In our study, amplitude and source location of the P200 reveal the timing and the putative structures where the higher-order process of solving the conflict between tactile and proprioceptive information is likely to take place. Despite the fact that illusory Aristotle and Reverse percepts were evoked by 1 and 2 objects, respectively, P200 amplitudes were comparable in these 2 conditions and were higher than in the Asynchronous control condition where 2 objects were used (Fig. 5). Interestingly, the latency of this effect on P200 is reminiscent of the time at which the process of remapping spatial coordinates takes place. Indeed, studies suggest that a somatotopic frame of reference prevails up to 60 ms after stimulus application, and a spatio-centered reference frame starts prevailing between 180 and 360 ms after stimulus onset (Craig and Busey 2003; Azañón and Soto-Faraco 2008; Azañón et al. 2010). The inferior parietal localization of the P200 components found in our study highlights the role of this structure in remapping touch when it conflicts with proprioceptive input. This is in line with the notion that the PPC subserves the multisensory processes that maintain and update the postural representation of the body (Snyder et al. 1998; Wolpert et al. 1998; Lloyd et al. 2003; Filimon et al. 2009).

Tactile stimulation delivered to crossed fingers gives rise to illusory perception because of the inherent conflict between the process of localizing tactile stimuli and coding the relative position of different body parts. Touch and proprioception are mapped closely in S1. However, the process of reshaping somatotopic maps according to the new unnatural fingers'

position that is necessary to tell apart illusions from reality (Benedetti 1985, 1986a, 1986b) does not occur in S1, but rather in the PPC where integration of tactile and proprioceptive information takes place. Indeed, the PPC, particularly on the left side, seems necessary for the integration of kinesthetic and haptic information during hand/object interactions. In particular, posterior parietal regions are involved in: (1) texture-based identification of objects through multifingers manipulation [when the integration of tactile inputs from each finger is strongly required (Roland et al. 1998; Deibert et al. 1999; Bodegard et al. 2001)]; (2) discrimination of 1 vs. 2 points (Akatsuka et al. 2008) or tactile recognition of objects moving on the fingers (Kitada et al. 2003); (3) illusory perception of hand movement when the hand holds an object (Naito and Ehrsson 2006). It is worth noting that multisensory integrative processes taking place in the PPC seem to be responsible also for the estimation of the size of objects touching the body, since changes in object size perception are induced by changing the visual size of tactually stimulated body parts (Taylor-Clarke et al. 2004; Longo and Haggard 2011).

It is also relevant that activity in the PPC is related to binding multimodal inputs, as indicated by a number of studies where integration of different sensory modalities brings to enhancement or attenuation of illusory perception. Indeed, the PPC is activated during kinesthetic illusions occurring under congruent bimodal proprioceptive–tactile stimulations with respect to the weaker illusions elicited under unimodal stimulation (Kavounoudias et al. 2008). The PPC is also involved during attenuation of illusory movement sensation elicited by tendon vibration when a live image of a participant's vibrated static hand conflicted with kinesthetic information that signals hand movement (Hagura et al. 2007). In addition, PPC activity is associated with recalibrating the perceived position of one's own hidden hand toward the visible rubber hand (Ehrsson et al. 2004). Lastly, the PPC is involved in illusory speech perception occurring when incongruent (when compared with congruent) audio-visual syllables are presented (such as in the mcGurk illusion; Benoit et al. 2010).

Thus, one additional point of novelty of our study is that PPC is also involved in resisting illusory perception resulting from within-modality tactuo-proprioceptive conflicting inputs coming from the body. Indeed, P200 amplitudes and source localization were different depending on whether subjects resisted or were prone to experience the Aristotle and Reverse illusions (Fig. 4). Significant negative correlations between P200 amplitude and indices of nonveridical perception (Fig. 5) indicate that larger posterior parietal positivity was involved in solving the conflict between tactile and proprioceptive inputs induced by fingers crossing. This remarkably implies that neural activity in higher-order posterior parietal cortices is specifically involved in solving the conflict between 2 different somatic submodalities, thus eliminating illusory percepts. In this perspective, the PPC may not simply be a multisensory convergence area, but it may be crucial for maintaining a coherent body image through suppression of multimodal conflicts.

Conclusion

In conclusion, the present findings highlight the spatio-temporal dynamics of brain activations during phenomenal susceptibility or resistance to somatosensory illusions deriving from the noncanonical alignment of touch and proprioception. Our results fit well with the notion that perception of tactile stimuli is modulated by multimodal feedback signals from higher-order associative cortices to primary somatosensory areas (Hochstein and Ahissar 2002; Driver and Noesselt 2008). In our experimental conditions, higher activity in the multisensory PPC correlated with the tendency to solve the conflict between tactile and proprioceptive somatic submodalities and, thus, may work as a "conflict resolver" that plays a suppressive influence on illusions and promote veridical perception. One may wonder why veridical perception is achieved only in some of the trials. Human and monkey studies indicate that, under conditions of perceptual uncertainty, such as in the case of near-threshold (de Lafuente and Romo 2005) or masked (Palva et al. 2005) stimuli, the nature of the resulting conscious percept depends on the fluctuation of neural activity not only in early sensory cortices, but also in higher-order multisensory parietal areas and in frontal regions (Deco and Romo 2008). Although our study was not devised to explore the role of large-scale connectivity in modulating conscious somatic percepts, the suggestion is made that inherent fluctuations of activity in the PPC make subjects more or less prone to somatosensory illusions.

Supplementary Material

Supplementary material can be found at: http://www.cercor.oxfordjournals.org/.

Notes

This study was funded by the EU Information and Communication Technologies grant (VERE project, FP7-ICT-2009-5, Prot. Num. 257695) and the Ministero Istruzione Università e Ricerca (Progetti di Ricerca di Interesse Nazionale, PRIN 2009). We thank to F. Zidda and A. Bultrini for their help in a preliminary phase of the study. *Conflict of Interest*: None declared.

References

Akatsuka K, Noguchi Y, Harada T, Sadato N, Kakigi R. 2008. Neural codes for somatosensory two-point discrimination in inferior parietal lobule: an fMRI study. Neuroimage. 40:852–858.

Allison T, McCarthy G, Wood CC, Darcey TM, Spencer DD, Williamson PD. 1989. Human cortical potentials evoked by stimulation of the median nerve. I. Cytoarchitectonic areas generating short-latency activity. J Neurophysiol. 3:694–710.

American Clinical Neurophysiology Society (ACNS). 2006. Guideline 9D: guidelines on short-latency somatosensory evoked potentials. J Clin Neurophysiol. 23:168–179.

Aristotle. 1924. Metaphysics. Oxford (UK): Oxford University Press.

Azañón E, Longo MR, Soto-Faraco S, Haggard P. 2010. The posterior parietal cortex remaps touch into external space. Curr Biol. 20:1304–1349.

Azañón E, Soto-Faraco S. 2008. Changing reference frames during the encoding of tactile events. Curr Biol. 18:1044–1049.

Benedetti F. 1991. Perceptual learning following a long-lasting tactile reversal. J Exp Psychol Hum Percept Perform. 17:267–277.

Benedetti F. 1985. Processing of tactile spatial information with crossed fingers. J Exp Psychol Hum Percept Perform. 11:517–525.

Benedetti F. 1986b. Spatial organization of the diplesthetic and nondiplesthetic areas of the fingers. Perception. 15:285–301.

Benedetti F. 1986a. Tactile diplopia (diplesthesia) on the human fingers. Perception. 15:83–91.

Benoit MM, Raij T, Lin FH, Jääskeläinen IP, Stufflebeam S. 2010. Primary and multisensory cortical activity is correlated with audiovisual percepts. Hum Brain Mapp. 31:526–538.
Blankenburg F, Ruff CC, Deichmann R, Rees G, Driver J. 2006. The cutaneous rabbit illusion affects human primary sensory cortex somatotropically. PLoS Biol. 4:e69.
Bodegård A, Geyer S, Grefkes C, Zilles K, Roland PE. 2001. Hierarchical processing of tactile shape in the human brain. Neuron. 31:317–328.
Chen LM, Friedman RM, Roe AW. 2003. Optical imaging of a tactile illusion in area 3b of the primary somatosensory cortex. Science. 302:881–885.
Chen LM, Turner GH, Friedman RM, Zhang N, Gore JC, Roe AW, Avison MJ. 2007. High-resolution maps of real and illusory tactile activation in primary somatosensory cortex in individual monkeys with functional magnetic resonance imaging and optical imaging. J Neurosci. 27:9181–9191.
Craig JC, Busey TA. 2003. The effect of motion on tactile and visual temporal order judgments. Percept Psychophys. 65:81–94.
Cruccu G, Aminoff MJ, Curio G, Guerit JM, Kakigi R, Mauguiere F, Rossini PM, Treede RD, Garcia-Larrea L. 2008. Recommendations for the clinical use of somatosensory-evoked potentials. Clin Neurophysiol. 119:1705–1719.
Deco G, Romo R. 2008. The role of fluctuations in perception. Trends Neurosci. 31:591–598.
Deibert E, Kraut M, Kremen S, Hart J Jr. 1999. Neural pathways in tactile object recognition. Neurology. 52:1413–1417.
de Lafuente V, Romo R. 2005. Neuronal correlates of subjective sensory experience. Nat Neurosci. 8:1698–1703.
Dieguez S, Mercier MR, Newby N, Blanke O. 2009. Feeling numbness for someone else's finger. Curr Biol. 19:R1108–9.
Driver J, Noesselt T. 2008. Multisensory interplay reveals crossmodal influences on "sensory-specific" brain regions, neural responses, and judgments. Neuron. 57:11–23.
Ehrsson HH, Spence C, Passingham RE. 2004. That's my hand! Activity in premotor cortex reflects feeling of ownership of a limb. Science. 305:875–877.
Filimon F, Nelson JD, Huang RS, Sereno MI. 2009. Multiple parietal reach regions in humans: cortical representations for visual and proprioceptive feedback during on-line reaching. J Neurosci. 29:2961–2971.
Gardner EP, Costanzo RM. 1980. Spatial integration of multiple-point stimuli in primary somatosensory cortical receptive fields of alert monkeys. J Neurophysiol. 43:420–443.
Gardner EP, Spencer WA. 1972. Sensory funneling. II. Cortical neuronal representation of patterned cutaneous stimuli. J Neurophysiol. 35:954–977.
Hagura N, Takei T, Hirose S, Aramaki Y, Matsumura M, Sadato N, Naito E. 2007. Activity in the posterior parietal cortex mediates visual dominance over kinesthesia. J Neurosci. 27:7047–7053.
Hashimoto I, Yoshikawa K, Sasaki M. 1988. Somatosensory evoked potential correlates of psychophysical magnitude estimations for tactile air-puff stimulation in man. Exp Brain Res. 73:459–469.
Hayward V. 2008. A brief taxonomy of tactile illusions and demonstrations that can be done in a hardware store. Brain Res Bull. 75:742–752.
Hochstein S, Ahissar M. 2002. View from the top: hierarchies and reverse hierarchies in the visual system. Neuron. 5:791–804.
Kavounoudias A, Roll JP, Anton JL, Nazarian B, Roth M, Roll R. 2008. Proprio-tactile integration for kinesthetic perception: an fMRI study. Neuropsychologia. 46:567–575.
Kitada R, Kochiyama T, Hashimoto T, Naito E, Matsumura M. 2003. Moving tactile stimuli of fingers are integrated in the intraparietal and inferior parietal cortices. Neuroreport. 14:719–724.
Lloyd DM, Shore DI, Spence C, Calvert GA. 2003. Multisensory representation of limb position in human premotor cortex. Nat Neurosci. 1:17–18.
Longo M, Haggard P. 2011. Weber's illusion and body shape: anisotropy of tactile size perception on the hand. J Exp Psychol Hum Percept Perform. 37:720–726.
Longo MR, Azañón E, Haggard P. 2010. More than skin deep: body representation beyond primary somatosensory cortex. Neuropsychologia. 48:655–668.
Luck SJ. 2005. An introduction to the event-related potential technique. CA (USA): MIT Press.
Macknik SL, Haglund MM. 1999. Optical images of visible and invisible percepts in the primary visual cortex of primates. Proc Natl Acad Sci USA. 96:15208–15210.
Naito E, Ehrsson HH. 2006. Somatic sensation of hand-object interactive movement is associated with activity in the left inferior parietal cortex. J Neurosci. 26:3783–3790.
Oldfield RC. 1971. The assessment and analysis of handedness: the Edinburgh inventory. Neuropsychologia. 9:97–113.
Palva S, Linkenkaer-Hansen K, Näätänen R, Palva JM. 2005. Early neural correlates of conscious somatosensory perception. J Neurosci. 25:5248–5258.
Penfield W, Boldrey E. 1937. Somatic motor and sensory representation in the cerebral cortex of man as studied by electrical stimulation. Brain. 60:389–443.
Rivers WHR. 1894. A modification of Aristotle's experiment. Mind. 3:583–584.
Roland PE, O'Sullivan B, Kawashima R. 1998. Shape and roughness activate different somatosensory areas in the human brain. Proc Natl Acad Sci USA. 95:3295–3300.
Shore DI, Spry E, Spence C. 2002. Confusing the mind by crossing the hands. Brain Res Cogn Brain Res. 1:153–163.
Simons SB, Chiu J, Favorov OV, Whitsel BL, Tommerdahl M. 2007. Duration-dependent response of SI to vibrotactile stimulation in squirrel monkey. J Neurophysiol. 97:2121–2129.
Snyder LH, Grieve KL, Brotchie P, Andersen RA. 1998. Separate body- and world-referenced representations of visual space in parietal cortex. Nature. 394:887–891.
Talairach J, Tournoux P. 1988. Co-planar stereotaxic atlas of the human brain. Stuttgart: Georg Thieme-Verlag.
Taylor-Clarke M, Jacobsen P, Haggard P. 2004. Keeping the world a constant size: object constancy in human touch. Nat Neurosci. 7:219–220.
Thomas DG, Grice JW, Najm-Briscoe RG, Miller JW. 2004. The influence of unequal numbers of trials on comparisons of average event related potentials. Dev Neuropsychol. 26:753–774.
Valeriani M, Le Pera D, Tonali P. 2001. Characterizing somatosensory evoked potential sources with dipole models: advantages and limitations. Muscle Nerve. 24:325–339.
von Bekesy G. 1967. Sensory inhibition. Princeton (NJ): Princeton University Press.
Whitney D, Goltz HC, Thomas CG, Gati JS, Menon RS, Goodale MA. 2003. Flexible retinotopy: motion-dependent position coding in the visual cortex. Science. 302:878–881.
Wolpert DM, Goodbody SJ, Husain M. 1998. Maintaining internal representations: the role of the human superior parietal lobe. Nat Neurosci. 1:529–533.
Yamamoto S, Kitazawa S. 2001. Reversal of subjective temporal order due to arm crossing. Nat Neurosci. 4:759–765.